Effects of Different Connection Types on Mechanical Behavior of Cross-lap Joints of *Phyllostachys makinoi* Culms

Dong-Ying Lee,[a] Min-Jay Chung,[a] Ming-Jer Tsai,[b] and Chia-Ju Lee [a,*]

Mechanical properties and behaviors of bamboo joined by different connections were considered in this work. Makino bamboo (*Phyllostachys makinoi*) culms from Taiwan were used as the connection material to explore the form of cross-lap joints. Since the cross-lap joint is a common joint in bamboo structures, the mechanical properties of tension, slip, and rotation were evaluated for three types of joints: lashing joint, iron wire joint, and steel bracket joint, under different load conditions. The results showed that the ultimate load of bamboo culms under lateral partial compression has a positive correlation with the number of bamboo nodes and the relative distance to the base-section of the bamboo culms. The mid-sections and end-sections have similar uniaxial compressions in the transverse orientation. According to results of tensile testing, the tensile stiffness of the three joint types is as follows in descending order: iron wire joint, lashing joint, and steel bracket joint, with the reverse order for ultimate load testing. In terms of slip testing, the withstanding of ultimate loads and increases in slip stiffness can be attributed to bamboo nodes that assist in creating slip stiffness in lashing joint. However, ultimately, steel bracket joints hold the highest slip stiffness. Our findings for rotation stiffness value show the following tendency: steel bracket joint > lashing joint > iron wire joint.

DOI: 10.15376/biores.19.4.7911-7930

Keywords: Phyllostachys makinoi; Bamboo joint; Cross lapping; Mechanical behavior

Contact information: a: Experimental Forest, National Taiwan University, No. 12, Section 1, Chien-Shan Road, Chu-Shan, Nantou Hsien, 55750, Taiwan; b: School of Forestry and Resource Conservation, National Taiwan University, Taipei 10617, Taiwan
** Corresponding author: chiaju@ntu.edu.tw*

INTRODUCTION

Bamboo is a fast-growing monocotyledon. When bamboo reaches growth of three to five years, it holds the optimal mechanical properties and is one of the earliest known wood fiber materials to be utilized for structural purposes. Because the cost of bamboo is low and yet it is versatile in application, it has been used in architectural columns, trusses, and as inner woven frames for mud-plastered walls (Raj and Agarwal 2014). When bamboo culms have the same density as timber, they show great mechanical properties and load capacity along with a modulus of elasticity (MOE) and relative curvature that surpass the properties of wood (Ahmad and Kamke 2005; Obataya *et al*. 2007). This indicates a high potential for developing bamboo for structural applications. Additionally, bamboo structures are mainly composed of linear bamboo culms. The connection between the

structural members can transmit and disperse the external force on the main frame. Thus, the type of joining method between bamboos greatly affects the strength of the bamboo structure as a system. Most commonly, there are three main ways of connecting bamboo: lengthening, merging, and joints. Vahanvati (2015) indicated that there are various types of affixation methods for bamboo culms including but not limited to: lashing, steel bolts, clamps, hubs along with brackets and plates, *etc*. However, there are also various types of bamboos corresponding to various types of material properties, and the affixation spot and method in addition to the corresponding bamboo species need to be considered to evaluate the structural properties of bamboos.

Amada and Untao (2001) revealed the facture toughness of bamboo fiber to be 116.2 MPa·$m^{1/2}$, which is evidently higher than those of commercial timbers such as spruce (7.0 MPa·$m^{1/2}$) and Southern pine (1.64 MPa·$m^{1/2}$). However, bamboo culms in growth do not have horizontal tissues; their vertical grain holds a fracture toughness ranging between 150 and 200 kPa·$m^{1/2}$, which is significantly lower than other materials. Thus, when bolts or nails are used as the joining method between bamboo culms, stress concentration is likely to occur due to the punctures, which make the bamboo susceptible to longitudinal splitting of the entire culm. If the aim is to maintain the bamboo culms' structural integrity, then it is ideal to use non-invasive methods such as iron wire or lashing for joining bamboo culms together. However, while steel bracket joints are liable to cause longitudinal splitting to the bamboo culm from the screws and bolts used, the assembly process is straightforward; thus the reputation of these joints as an easy-to-assemble method is gaining momentum in the bamboo construction industry. Moran *et al.* (2016) targeted research on the point of contact of metal brackets and fastenings for their mechanical properties. The research showed that when the bamboo culm is encased by a metal bracket part, it can effectively minimize longitudinal splitting. Additionally, metal is a homogenous material, and simulation tests analyze the integrity of the various metal connections' assembly and contact with the building material. Metal parts and fastenings are easier to assemble than lashing, and they have potential to be utilized for their strength and the further design of metal parts.

Iron wire and rope use rope-form materials to lash two or more culms to secure them in place. Because iron wire and ropes are easy to acquire and form together without limitations, the production team only needs simple knowledge about winding and lashing to assemble temporary or light structures such as scaffolds and fences. After design and planning, it is possible to produce geometrical and large spanning structures. Additionally, when the joint is damaged or deteriorated, the iron wire and rope can be replaced without removing the main structure components, which could possibly compromise the integrity and increase the lifespan of bamboo culms. While there has been little research about the mechanical properties of lashing and iron wire joint, there has been more research regarding the strength and the reinforcing effect on the strength and rigidity of the connection (Awaludin and Andriani 2014; Hong *et al*. 2020).

Makino bamboo is commonly used as a building material for bamboo canopies, and the cross-lap joint is a commonly used joint in connecting bamboo culms. In this study, cross-lap joints were used as the connection construction method. Nylon rope and iron wire are selected as the test example of the lashing method and the specimen of the metal fitting method is the steel angle bracket. This study investigated their mechanical properties, including tension, slip and rotation, to evaluate the failure modes, mechanical behaviors, and limitations of the three joint types under load.

EXPERIMENTAL

Materials

This study utilized four-year-old makino bamboo (*P. makinoi* Hayata) from Taiwan with a diameter of 5 to 6 cm and a total length between 145 and 150 cm. Because the bamboo wall thickness and its growth length hold an inverse relationship, the end section of bamboo culm has longer distance between nodes and thinner walls. Conversely, the basic section of bamboo culm closing to the ground has shorter distance between nodes and thicker walls. The specimens of bamboo culm were cut into equal lengths corresponding to the following length: 30 cm of basic-section, 30 cm of mid-section and 30 cm of the end-section (Fig. 1). These bamboo culms were placed in a constant temperature and humidity chamber at 20 °C, 65% relative humidity for 7 days to achieve moisture equilibration.

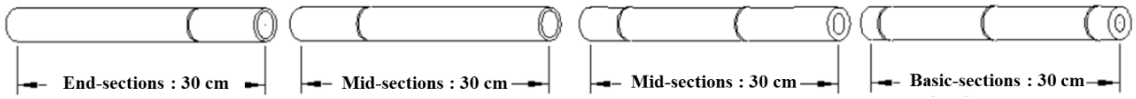

Fig. 1. Sampling of bamboo culms

The lashing rope was chosen primarily due to its composition of polypropylene and polyethylene and its diameter is 3.0 mm with ultimate tensile load of 84 kgf, and the length of rope is 3000 mm. The iron wire used for the iron wire joint is galvanized steel wire with a diameter of 2.0 mm. The length of wire is 2000 mm with an ultimate tensile load of 103.5 kgf. The metal fittings used in the steel bracket joint are made of galvanized low carbon steel with an angle of 90°, and there are four holes on both sides of the bracket. The size of bracket is 35 x 35 cm with a thickness of 1.5 mm.

Methods

Immediately after sample extraction, the bamboo culms were placed in a controlled environment for 14 days under 20 °C at 65% RH. After the bamboo's moisture levels were adjusted, the weight and thickness of the bamboo culm walls were measured and the culms would be further classified. This study examined the cross-lap joint configuration. Figure 2 shows the cross-lap joint configuration where two bamboo culms cross over each other on a perpendicular angle with the indication that the securing methods are subject to variation. The ultimate tensile load and the slip ultimate load of the two bamboo culms were used as the basis to evaluate the joint axial forces. The deflection caused by rotation conducted through rotation tests was used as the strength index. The stiffness between the bamboo culms shows the ability of joint to resist torsion and deformation, usually expressed by the external force required to produce a unit deformation. Additionally, this study established a linear regression model and drew a regression line from the mechanical curve of each test. The slope of the regression line was used as the stiffness value of the test. The strength of the joint indicates the limit of the joint's resistance to the load. Therefore, both the tensile test and the slip test used the load value (kgf) of the first response load drop of the joints as the strength indicator. After the testing, the data were sorted and tabulated for analysis.

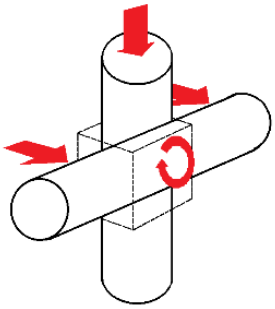

Fig. 2. Force situations of cross-lap

Lateral partial compression test

Lateral partial compression tests were used to evaluate the impact of bamboo culm quantities and their distribution on the bamboo specimen; subsequently, their properties and characteristics were used to categorize them. The categories were as follows: no node, one node, and three nodes, as shown in Fig. 3. In the initial stages of cutting, the bamboo culms were all already oriented according to their direction of growth; thus, it is easier to cut and categorize according to the base section, mid-section and end-section. Due to these categorizations, the average quantity of nodes also varied between the bamboo part categories. Since each control specimen was tested repeatedly ten times, ninety sets of test specimen were required.

Fig. 3. None-node compression specimen (a), one-node compression specimen (b), two-node compression specimen (c)

Fig. 4. Lateral partial compression test

Figure 4 shows the specifications of the universal strength testing machine used to conduct the tests: Shimadzu UH-10A, Japan. To conduct strength tests, the specimens were placed on the platform along with a metal slab measuring 20 cm × 5 cm × 2 cm (L × W × D) to assist with load concentration. In the trial run, the loading rate speed was set to 2 mm/min and retained until the load rate decreased or the test material was crushed; The ultimate load (P_u) values were recorded.

Preparation of joint

This study utilized square lashing as its primary lashing technique, as shown in Fig. 5. The lashing was fixed with a rope tension of 16 to 17 kgf. As depicted in Fig. 6, iron wire tying took on a single cross-over point between two bamboo culms. Figure 7(c) shows that in steel bracket bracing, the central alignment between the two bamboo culms was secured first by screwing holes using a 2.5 mm diameter screw head and then tightening the screws after repositioning the brackets. Each side was fixed with 2 screws on bamboo culm to ensure it wouldn't come loose. Figure 7(c) indicates that the node positions on the bamboo did not interfere with bracket installation.

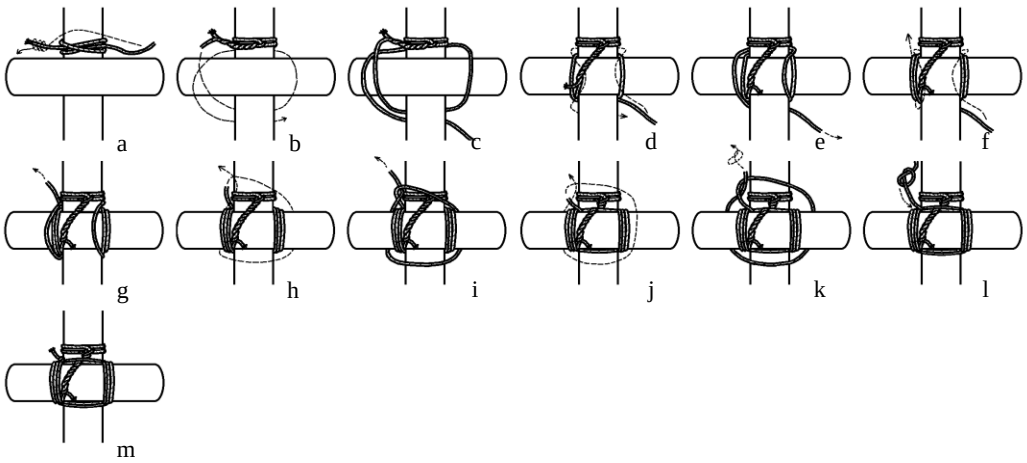

Fig. 5. Lashing process of square lashing joint

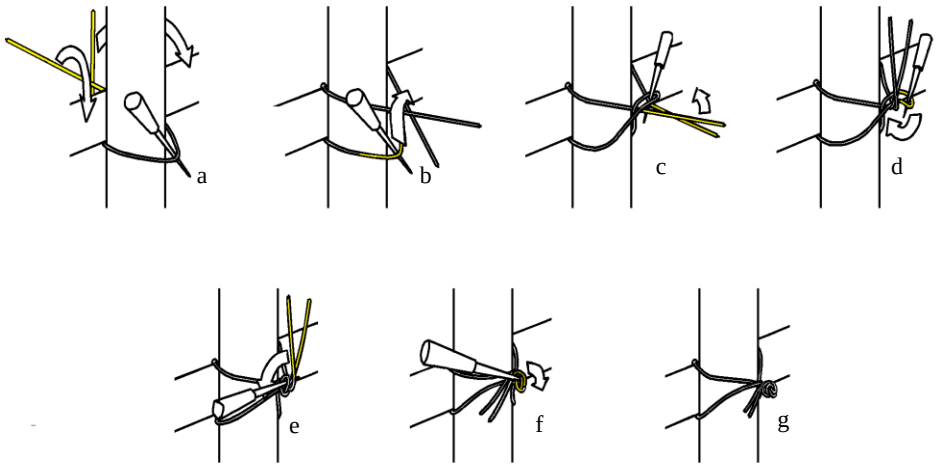

Fig. 6. Fixing process of iron wire joint

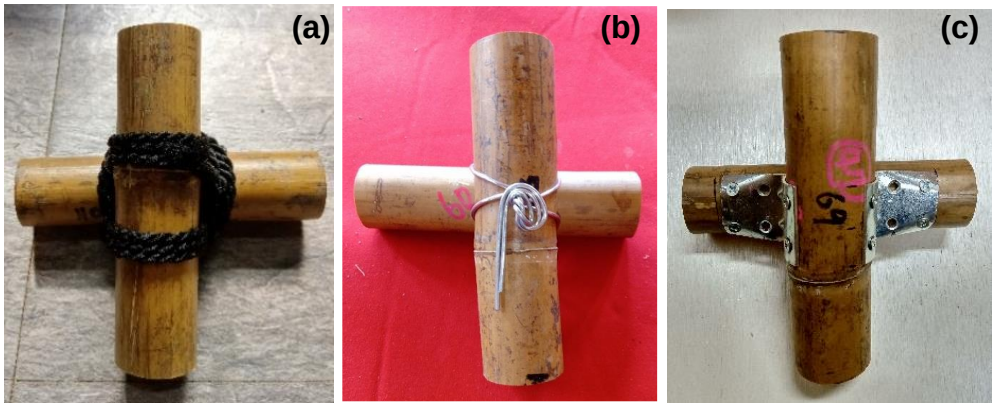

Fig. 7. Specimen of lashing joint (a), iron wire joint (b), and steel angle bracket joint (c)

Tensile test

The stretch tests determine the ultimate tensile value (P_u) and failure mode. The tensile test specimen of the three joint types were all derived from the end or the mid-section of the bamboo culms that were placed in a perpendicular, cross-over configuration. Studies conducted by Chand *et al.* (2008) indicate that the fibers closer to the bamboo node are shorter and higher in density and thus exhibit higher sheer strength. The three different test materials all contained a bamboo node; however, the node did not impact the lashing or steel bracket installation. Figure 8 (a) shows the tensile testing load as an inverted U-shaped load on the universal strength testing machine. The test material was placed on two horizontal Y-shaped carriers with a loading rate of 15 mm/min and its results were recorded when the inverted U-shape load comes in contact with the bamboo culms. The loading rate was maintained until the reaction load dropped to 50% of the ultimate load (P_u) or until the rope broke; this was the extent of recording the P_u and the load displacement.

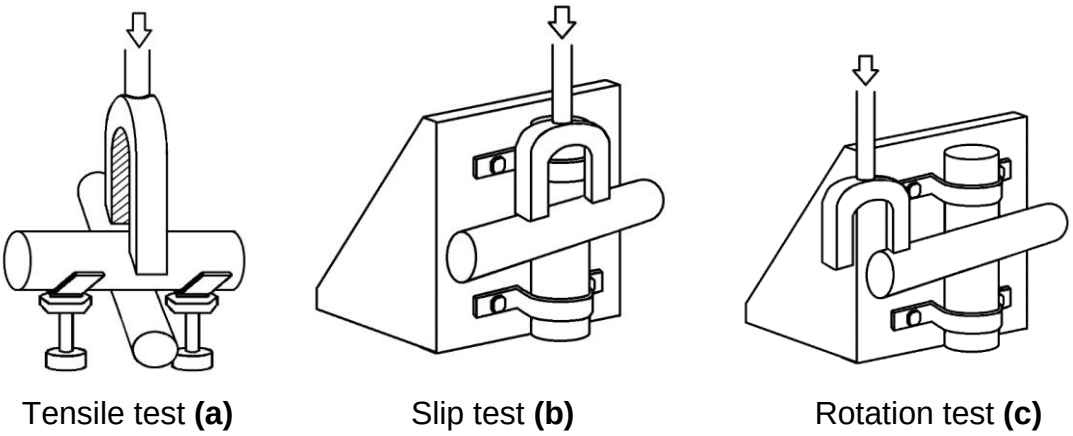

Fig. 8. Test methods of tensile, slip and rotation

Slip test

The test specimen for the slip test comprises two mid-section bamboo culms measuring 30 cm. The securing method is depicted in Fig. 8 (b), which shows a metal bracket as the contact point for installation, which transversely coincides to the load. A loading rate of 15 mm/min was maintained until the reaction load suddenly dropped to 50% of the ultimate load or the bamboo culm broke and halted thereafter. The results for the ultimate load (P_u) and the load were recorded.

Rotation test

Like the test specimen used in slip test, the specimen for the rotation tests also used two mid-section bamboo culms measuring 30 cm. The configuration and securing methods are shown in Fig. 8 (c), which shows a clamp adjusted to an inverted U-shaped load. One end of the horizontal culm acted as the lever arm measuring 11 cm from the joint. The rotation test used a loading rate of 15 mm/min and the testing stopped after the load had a vertical displacement of 10 cm or the joint was damaged. The entire process was filmed in order to record the displacement and rotation angle, as seen in Fig. 9, which shows the lever arm and rotation angle diagram; the bending moment of the rotation angle was determined by multiplying the rotation of the 11 cm lever arm by the load value (kgf) corresponding to the different rotation angle.

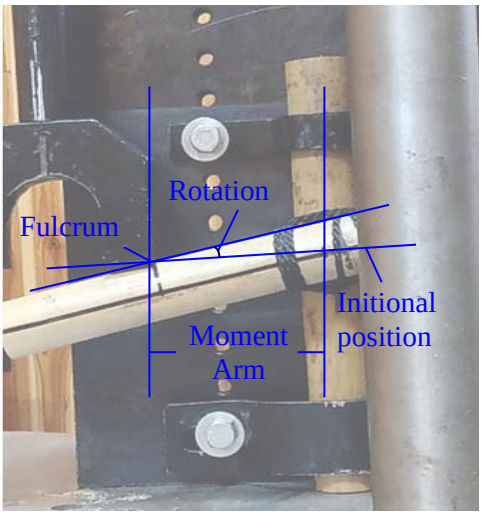

Fig. 9. Moment arm and rotation angle

Analysis of variance

Data are presented as the mean of nine replicates with standard deviation (SD, presented in parentheses). Differences between experimental specimens were examined using Tukey's test and analysis of variance (ANOVA) with $p < 0.05$ indicating statistically significant difference. All analyses were performed using the software Statistical Analysis System (SAS Institute Inc., NC, USA) 8.0.

RESULTS AND DISCUSSION

Lateral Partial Compression Test

Figure 10 (a) shows the failure mode for specimens without nodes that were fragmented into four pieces, while Fig. 10 (b) and (c) show bamboo culms with a single node and Fig. 10 (d) and (e) show bamboo culms with two nodes that were not split into four parts due to the presence of bamboo nodes. However, according to the cross-section of the three types of specimens seen from the end, each specimen was fractured along the line perpendicular to the load; which indicates that the three types of specimens all underwent the same stress distribution when subject to the same type of external forces. In bamboo culm with one node, the failure mode on the end aligned a parallel load direction fractures the bamboo culm from the internal wall to the external wall. In contrast, the failure mode of transverse load direction caused bamboo culm to split from the outer walls to the inner walls.

Research conducted by Kobayashi *et al.* (1996) regarding lateral load forces on brittle round tube suggested that tensile and compressive stress occurs on the top and bottom as well as on the left and right of the tube. The stress distribution on the left and right sides are divided into internal compression and external tension, while the forces on the top undergo outer compression and the bottom forces undergo internal tension. Since there are no horizontal fibers in the culm between the nodes, compared to compressive forces, tensile force is more likely to cause breakage between the fibers. This shows that when bamboo culms undergo perpendicular forces, they become fractured. The fractures that run in parallel to the bamboo culm fibers indicate a severe decline in load bearing

properties. Once the bamboo culm splits into two semi-circular forms under parallel load forces, the internal tensile force causes the circular structure to split and thus the bamboo culm loses its load bearing properties.

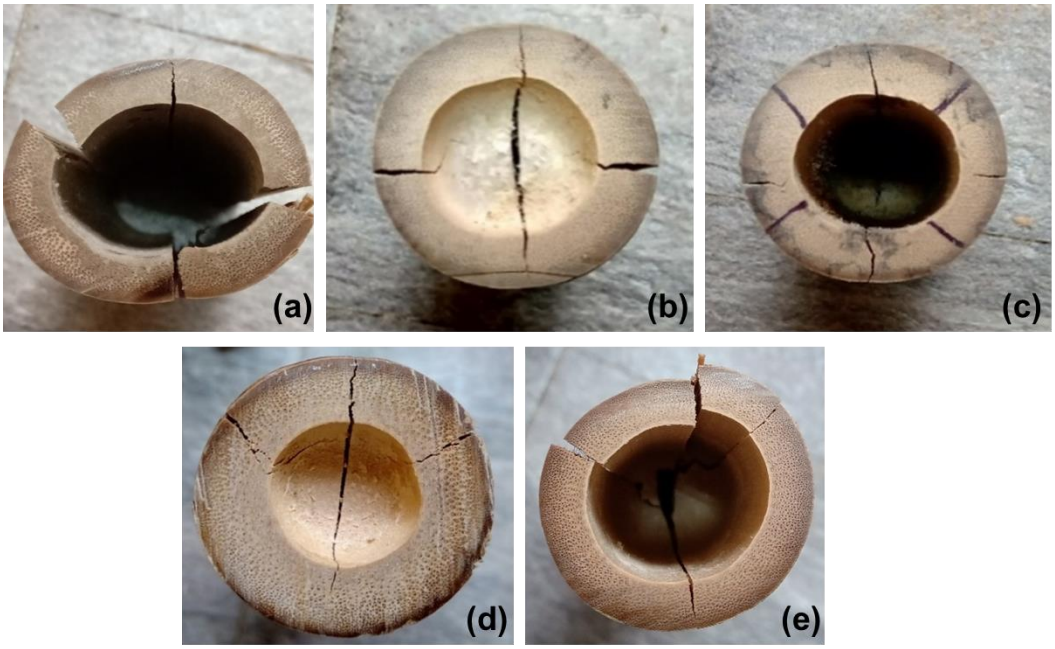

Fig. 10. Failure mode of none-node compression specimen (a), two ends in one-node compression specimen (b) and (c), two ends in two-node compression specimen (d) and (e)

Table 1. Results of Lateral Partial Compression Test

Number of Nodes	Sampling Position	Ultimate Load (kgf)
0	Base	405.56 ± 43.85^{a}
	Mid	280.36 ± 78.49^{bc}
	End	290.88 ± 71.51^{bd}
1	Base	532.84 ± 109.04^{e}
	Mid	323.32 ± 25.44^{cf}
	End	304.76 ± 59.99^{df}
2	Base	668.55 ± 117.37^{e}
	Mid	396.32 ± 91.27^{g}
	End	355.95 ± 117.0^{g}

Note: Results are mean ± S.D., n = 10; numbers followed by different letters (a-g) are statistically different at the probability level of $p < 0.05$ according to Tukey's test and ANOVA.

Table 1 shows the fractures along the edge of bamboo culms with variations in the number of nodes. When these culms are subject to compressive forces, the more nodes the bamboo culm has, the greater its ability to withstand ultimate load. When sampling position are closer to the end of the bamboo culm, its ability to withstand ultimate load decreases. This occurrence coincides with the ANOVA analysis and Tukey's tests that were conducted by Lee *et al.* (2020). The results showed that there were no significant differences in terms of ultimate loads across mid-section and end-section bamboo culms with no nodes, one node or two nodes. This suggests that mid-section and end-section makino bamboo culms have similar ability to resist lateral partial compressive force.

Henceforth, all subsequent specimens will use the mid-section or end-section of bamboo culm as the sampling position.

Tensile Test

Figure 11(a) conveys the failure mode for the tensile tests in three different joint types. The failure mode of the lashing joint is mainly a result of the bamboo culm crushed by compression. The cross-sectional failure on the bamboo culm ends holds the same outcome as the transverse compression test, which results in cracking into quadrants. This shows that the stress distribution generated during the tensile test is similar to the lateral partial compression test. Conversely, the tensile test did not produce any damage to the rope, indicating that the tensile stress of the rope was greater than the crushing load on the bamboo culm. Thus, the compressive properties of the bamboo culm can be used to illustrate the tensile properties of the lashing joint. Figure 11(b) shows that the failure mode of the iron wire joint was mainly due to untwist and loose the iron wire knot, which resulted in a loss of load capacity. The testing process on iron wire joint shows that while the iron wire experienced damage, no destruction was incurred on the bamboo culm. Meanwhile the failure mode on the bamboo culm connected by steel bracket showed that the non-compressed bamboo culms split longitudinally, thus losing load capacity.

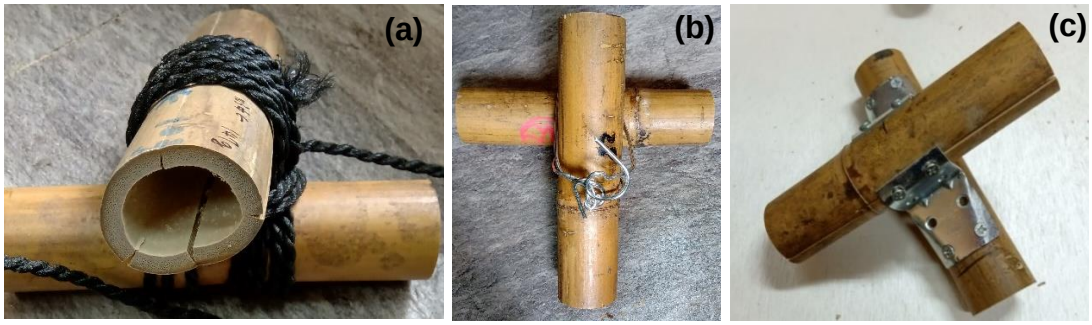

Fig. 11. Failure mode of tensile test in lashing joint(a), iron wire joint(b) and steel angle bracket joint(c)

In Fig. 11 (c), when the steel bracket joint between the two bamboo culms undergoes load, it causes the screw to loosen and produces vertical fiber tensile stress on the bamboo culm causing the bamboo culm to split; thus, the joint is no longer able to withstand the load. The ultimate load of the joint depends on the ability of the bamboo culm to resist the tensile stress of the vertical fiber. Therefore, regarding the tensile test, in the lashing joint and steel bracket joint, the bamboo culm's mechanical properties are what need to be reconsidered; while in the iron wire joint, the iron wire and subsequently the strength of the tying method are what need to be considered.

In Fig. 12 (a), as the load increases, the load-displacement curve of lashing joint also rises in a linear pattern; and the load drops suddenly after the point of failure. These findings align with those of Lee *et al*. (2020) and demonstrate that the load and displacement of the lashing joint are proportional to the amount of displacement during the tensile stress, which can be regarded as the elastic area of the joint and the slope of the curve in the linear interval can be regarded as the joint's tensile stiffness. From Fig. 12 (b) and (c), it can be seen that the load displacement curve of the iron wire joint and the steel bracket joint had a similar pattern. However, the curves of the latter two joint types, namely

lashing and iron wire joint, had the tendency to deter the ascending pattern after they surpassed the elastic area. This is an indication that the joint has entered plastic deformation and cannot return to its original material properties; and the lashing joint is crushed before the rope begins to deform when the bamboo culm has already faced breakage. Thus in stopping the experiment, the curve does not display an arcing pattern. In the three joint types, the only joint type of the three to face damage without breakage of the bamboo culms is the iron wire joint, which indicates that the plastic deformation is mainly provided by the iron wires.

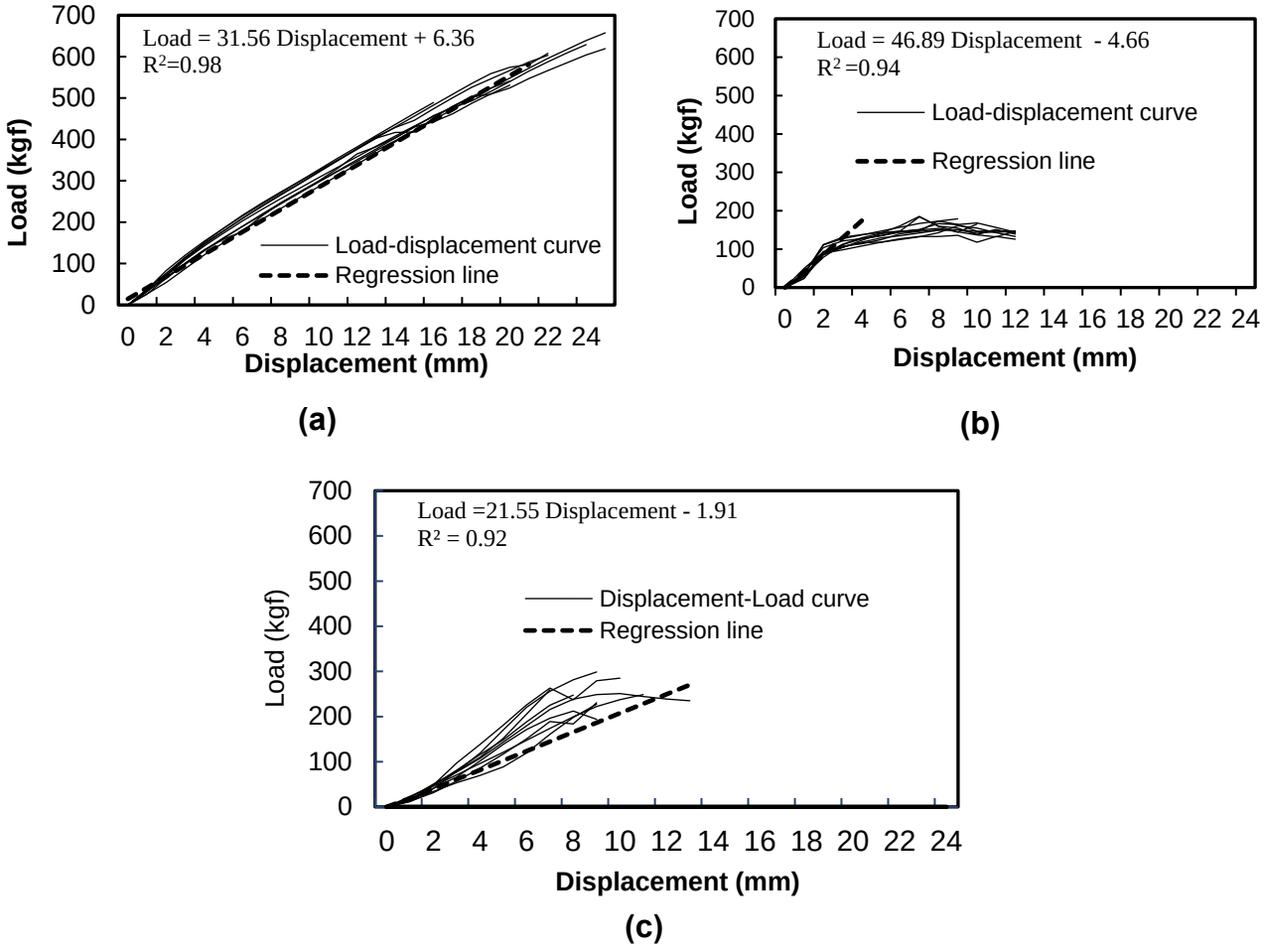

Fig. 12. Load-displacement curves of tensile test in lashing joint(a), iron wire joint(b) and steel angle bracket joint(c)

To explore the mechanical behavior of the three joint types under load, this study took the following specifications of joint materials: rope (0 to 9 mm), iron wire (0 to 2 mm), and steel bracket (0 to 2 mm) as the displacement ranges to construct a linear regression model and used the slope of the regression formula to represent the tensile stiffness of the joint. Figure 12 (a), (b) and (c) indicate that the tensile stiffness values of the three types of joint were in the following order: iron wire joint > lashing joint > steel bracket joint, signifying that within the elastic area, the resistance of the iron wire joint to tensile deformation is the highest among the three types of joint and once it passes through

the linear region, the load capacity of the joint drops significantly.

Table 2 compares the ultimate load and ultimate displacement of the three joint types. In descending order according to ability to withstand ultimate load they are ranked as follows: lashing joint, steel bracket joint and iron wire joint. In terms of the ultimate displacement, it can be seen that the lashing joint better-withstands the iron wire joint and the steel bracket joint and is thus statistically-verified in ANOVA, which confirms that the ultimate displacements of the iron wire joint and the steel bracket joint do not differ significantly. The findings show that the lashing joint can accept a larger load before the ultimate tensile load. Furthermore, the displacement of the bamboo culm before breaking for the lashing joint is greater than those of the iron wire and steel bracket joint. Although the tensile stiffness of the steel bracket joint is lower than iron wire joint, the ultimate load of the steel bracket joint is better than the iron wire joint under the same ultimate displacement; this indicates that of all three joints, the iron wire joint holds the lowest ultimate tensile strength.

Table 2. Results of Tensile Test

Type of Joint	Number of Tests	Ultimate Load P_u (kgf)	Ultimate Displacement (mm)	Failure Mode
Iron wire	10	172.99 ± 15.98[a]	9 ± 1.75[a]	Knot loosening
Lashing	9	616 ± 73.73[b]	23.39 ± 4.55[b]	Culm crushing
Steel angle bracket	9	262.41 ± 28.41[c]	9.17 ± 1.39[a]	Shear fracture in bamboo culm

Note: Results are mean ± S.D.; numbers followed by different letters (a-c) are statistically different at the probability level of $p < 0.05$ according to Tukey's test and ANOVA.

Slip Test

Figure 13(a) shows that regarding the load capacity of the lashing joint, a specimen with a bamboo node secured by one to two loops of lashing will lose load capacity immediately. Conversely, a specimen without a node did not have a sudden drop in load capacity. Thus, when the horizontal bamboo culm slides beneath the clamp, the clamp below is the stop factor of the test; these results align with the findings of Lee *et al.* (2020). Figure 13 (b) illustrates that on a bamboo specimen with a node secured by an iron wire joint, the enlarged deformation of the iron wire occurred after it slipped past the bamboo node, resulting in loss of load and indicating the failure mode of the test. For the iron wire joint on bamboo culm without node, the same result occurred for specimen without node in lashing joint. There were two types of failure modes in the steel bracket joint. Figure 13 (c) and (d) depict that the screws on the vertical side have loosened; the same occurred with the screws on the horizontal culm, which caused cleavage fractures along the horizontal bamboo culm.

Fig. 13. Failure mode of slip test in a lashing joint with node (a), iron wire joint (b) and steel angle bracket joint (c and d)

It is hypothesized that both types of failure modes can be attributed to mechanical properties such as wall thickness, bamboo density; these factors help the bamboo culms resist against the damages caused by the screws. If the horizontal culm's ability to resist against vertical fiber stress is poor, splitting will occur by default. Otherwise, the screws will break out of the vertical culms. Thus, the failure mode result of the slip test depends on the horizontal member's ability to resist splitting and the bamboo culm wall's ability to keep the screw from falling out.

Figure 14 (a) and (b) depict the load bearing properties as displacement curves of the lashing joint between bamboo culms with and without node.

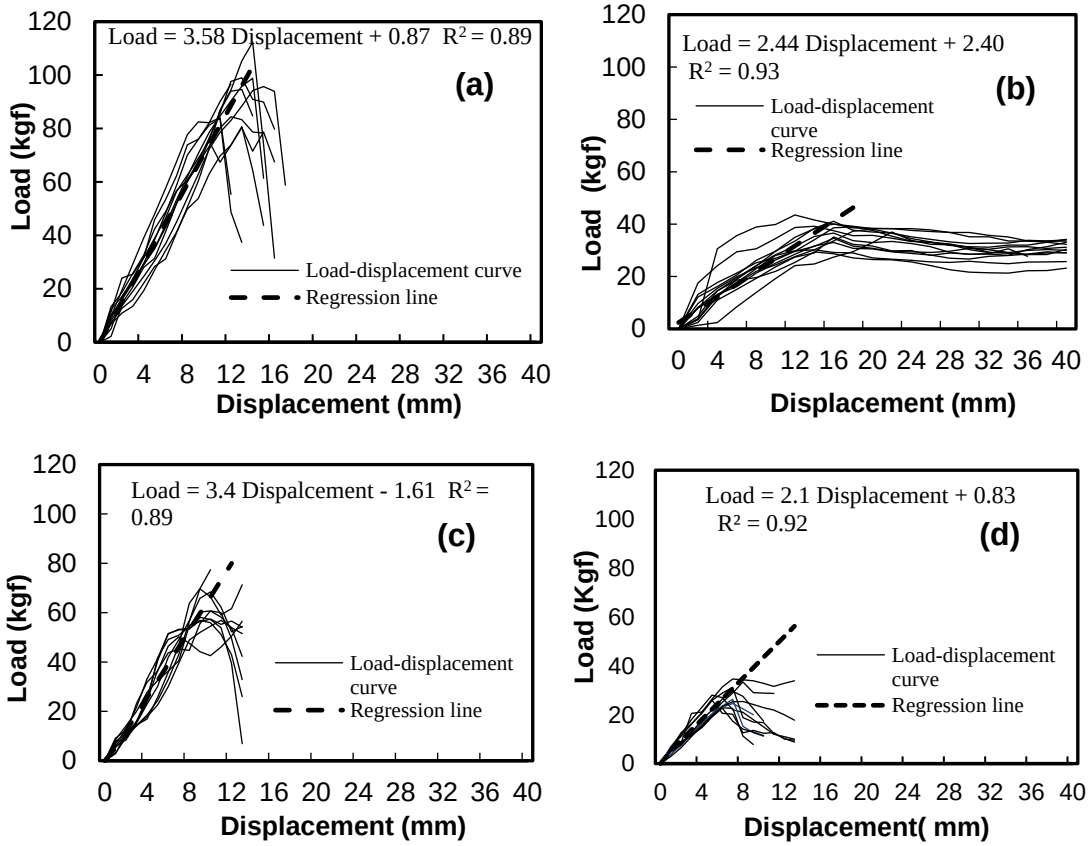

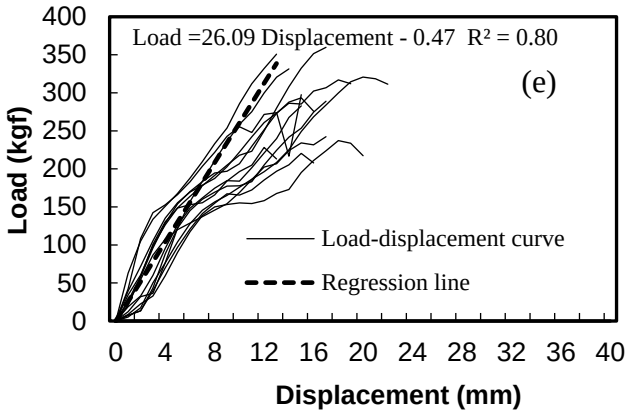

Fig. 14. Load-displacement curves of slip test in lashing joint with node(a), lashing joint without node(b), iron wire joint with node(c), iron wire joint without node(d) and steel angle bracket joint(e)

The results show that in regards to the load bearing properties of specimen with node, the load displacement curve held a linear relationship. This is reflected in the lashing joint. When the rope slipped through the bamboo node, the curve dropped immediately. Conversely, specimens without bamboo node also rose in a linear pattern. However, when the load became stabilized, the load capacity decreased and had difficulty ascending further. In another test, the fixed load value was maintained until the testing stopped. Because no rope breakage occurred throughout the testing processes, this indicates that the tensile strength of the rope was greater than the maximum static friction on the bamboo culm's surface, hence causing slippage in the lashing joint whilst maintaining a fixed load value. Figure 14 (c) and (d) respectively show the load displacement curve of the iron wire joint on culm-containing bamboo and of another bamboo specimen without a node; both had the same elastic area in lashing joint. When the elastic area was surpassed on the specimen with node, the curve faced a pattern of decline, which shows that the iron wire underwent a plastic state of torsion. Once the iron wire joint had surpassed the bamboo node, it reflected the tendency for the load capacity to decline. The load displacement curve for the specimen without node fixed by iron wire showed two main patterns: 1. The curve showed a gradual decline with no inclination of ascension. 2. The curve maintained a stable load bearing value until the end of test. It is hypothesized that both factors can be attributed to the iron wire joint's torsion and change in form. If the change in form of the iron wire joint was not as severe prior to slipping, the joint could still maintain a fixed reaction load; otherwise, its reaction load gradually decreased until it lost its load capacity, indicating that the presence of the bamboo node was able to alter the joint's mechanical behavior during load bearing. Figure 14 (e) shows the load displacement diagram of the steel bracket joint. The figure shows the displacement at the initial stage of 1 to 2 mm. The curve of each group of test materials increased in ascension in a divergent form. However, at the displacement range of 6 mm, each type of test specimen's displacement range had the tendency to shrink, which caused the deceleration of the curve mirroring a sharp drop in reaction load. This phenomenon suggests that in all of the specimens, their subsequent joint underwent plastic deformation, detachment or cracking. Thus, the subsequent mechanical behavior cannot be predicted.

In this experiment, the 0 to 12 mm displacement range was used as the linear interval of the curve in lashing joint and iron wire joint. Meanwhile the steel bracket joint

was established in its linear regression model a displacement range of 0 to 6 mm; the slope of the regression model indicates the slip stiffness of each joint. In Fig. 14, the slip stiffness of the five test materials can be observed in the following descending order: steel bracket joint > lashing joint with node > steel bracket joint with node > lashing joint without node > iron wire joint without node. By examining the interaction of the linear model of each joint, it can be seen that there was no significant difference in the slipping stiffness in the lashing joint and iron wire joint ($p > 0.05$). This indicates that the presence of bamboo node not only can improve the slipping stiffness of the lashing joint and the iron wire joint, but also it can produce similar slipping properties in elastic area. Due to the screws, the resistance of the steel bracket joint against slipping was much higher than the other two joints. However, at the same time, there is also vulnerability of bamboo culms to split after impact of load.

Table 3 compares the results of the ultimate load, ultimate displacement, and failure mode of the specimens. Through the ANOVA verification, no significant differences between the two failure modes of ultimate load and ultimate displacement in the steel bracket joint was present. This suggests that although there are different failure modes, the slip ultimate load of the steel bracket joint is about 295 kgf and has a fixed ultimate displacement. Meanwhile the slipping ultimate load in descending order is: steel bracket joint > lashing joint with node > iron wire joint with node > lashing joint without node > iron wire joint without node. This reveals that the extent to which the infiltration of the screw increases the resistance to slippage surpasses that of the existence of bamboo node; which have been shown to increase the limit of resistance to slippage. In contrast, the displacement of the iron wire joint is significantly greater than the other two types of joint. If the iron wire joint is utilized in structural applications, the risk of displacement is small in consideration of the ultimate load, yet the risk of displacement is large in consideration of joint deformation.

Table 3. Results of Slip Test

Type of Joint	With Node or not	Numbers of Tests	Ultimate Load P_u (kgf)	Ultimate Displacement (mm)	Failure Mode
Steel angle bracket	-	8	294.51 ± 33.28[a]	16.78 ± 2.62[a]	Screw out from vertical culm
	-	5	301.44 ± 67.46[a]	15.13 ± 1.47[a]	Screw out from horizontal culm
Iron wire	Yes	10	61.52 ± 7.56[b]	19.00 ± 2.36[b]	Wire loop slips through the node
	No	11	29.79 ± 3.55[c]	13.93 ± 2.55[c]	-
Lashing	Yes	11	96.18 ± 9.88[d]	27.11 ± 2.82[d]	Rope loop slips through the node
	No	11	38.73 ± 3.60[e]	15.49 ± 1.92[a]	-

Note: Results are mean ± S.D.; numbers followed by different letters (a-e) are statistically different at the probability level of p < 0.05 according to Tukey's test and A NOVA.

Rotation Test

Figure 15 shows the failure nodes of the three types of joints from rotation test. After the test, the horizontal bamboo culms received the most rotational impact in the lashing joint and iron wire joint. The vertical culms displaced within the range of 10 cm

however did not undergo any damage. Thus, the ultimate load (P_u) was not obtained in the test.

While the iron wire joint produced a severe extent of deformation of the knot without direct damage to the bamboo culm, the steel bracket joint caused the bamboo culm to be damaged through the separation of the horizontal bamboo culm and the splitting from the screw's insertion point. Because there was no sudden drop in the reaction load during testing, the ultimate load could not be obtained by these specimens.

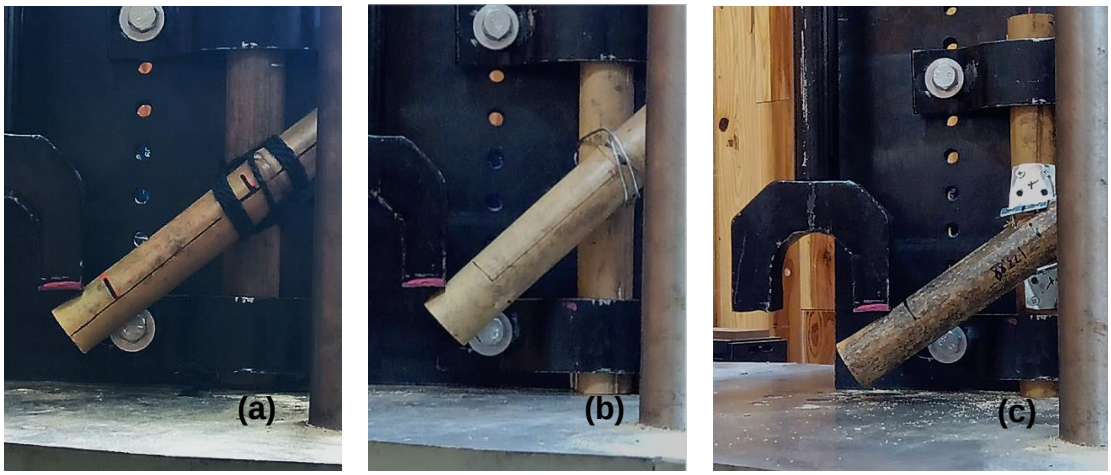

Fig. 15. Failure mode of rotation test in lashing joint (a), iron wire joint (b) and steel angle bracket joint(c)

Figure 16 shows the moment-rotation curves of the various joint types: (a) lashing joint, (b) iron wire joint, and (c) steel bracket joint. The curves of all three types of joint exhibited linear intervals during the initial stages of testing; the linear intervals show that the bending moments and the rotation angles at the initial stage of rotation were all proportional to each other, which indicates the elastic area of the joint.

After passing through the elastic area, the linear intervals could not return to their original position, which signifies that the loads on the joint had entered the plastic area. The curves of the iron wire joint and steel bracket joint still showed linear tendencies with different slopes after passing through the elastic area, while the curve line of the lashing joint aligns with a previous study (Lee *et al.* 2020) that used 0 to 0.25 radians, 0 to 0.03 radians, and 0 to 0.03 radians as the linear interval of the initial rotation angle for lashing joint, iron wire joint, and steel bracket joint, respectively. In the later stages, the rotation angle intervals of 0.1 to 0.4 radian and 0.04 to 0.2 radian were used as the linear interval of the iron wire joint and the steel bracket joint correspondingly to establish the linear regression model. The slope of the initial regression model represents the rotation stiffness of the three types of joint.

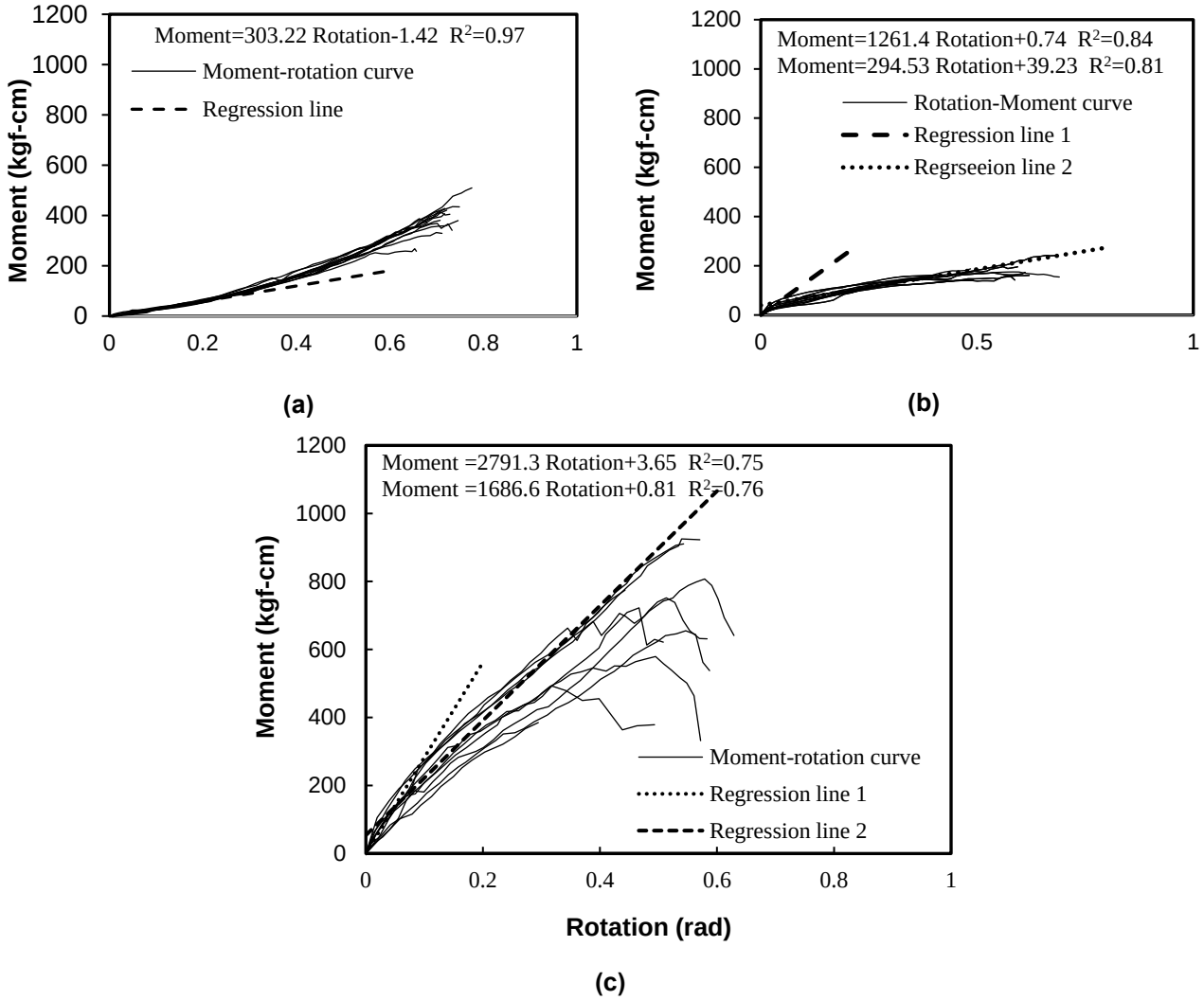

Fig. 16. Moment-rotation curves of lashing joint (a), iron wire joint (b) and steel angle bracket joint (c)

The initial rotational stiffness value of the iron wire joint was approximately 4.3 times the slope of the later regression model, indicating that the ability of the joint to resist rotational deformation was greatly reduced. Although the curve of the joint was linear in the later stages, the assumption is that the iron wire was embedded into the bamboo culm's walls due to the rotation process, which caused tightening of the iron wire around the bamboo. The ability of the bamboo culm's walls to resist the deformation caused by their embedment further affects the curve direction, leading to a linear tendency. All in all, the iron wire exhibited obvious plastic deformation and could not restore the horizontal member to its original position. Therefore, the slope of the late regression model cannot be simply regarded as the joint's rotational stiffness. The same applies to the steel bracket joint in which the initial rotation stiffness value was about 2.4 times the slope of the regression line at the later stage. This indicates that the steel bracket begins plastic deformation after rotating at a small angle and is unable to restore to its original condition. Although the curve in the later stage is linear, the speculated reason presented is because the bamboo culm walls resist the deformation caused by the screw falling out, which

subsequently affects the security of the steel bracket, and thus, the later slope cannot be regarded as the rotational stiffness.

Comparing the rotation stiffness results of the three joint types, it can be seen that the steel bracket joint held a significantly higher rotation stiffness than the other two joint types, signifying the bending moment that the steel bracket joint was able to endure the unit rotation angle in the elastic region is the highest of the three joint types. Additionally, the slope of the later regression model of the steel bracket joint (1686.6 kgf-cm rad^{-1}) was also higher than the rotational stiffness of the wire joint (1261.4 kgf-cm rad^{-1}). This shows that even if the steel bracket began to deform plastically during testing, its ability to resist rotation was still higher than that of a non-deformed iron wire joint. However, during the rotation test, the bamboo culm with the steel bracket joint was most susceptible to splitting due to the screw falling out. While all three joint types showed the tendency for the bamboo to split during the rotation test, the steel bracket joint was the most likely to cause the bamboo culm to fracture. This shows that the ability of joint to resist rotation was higher than the ability of the joint to attach to the bamboo culm, so the probability of the bamboo culm being damaged increased. Therefore, in addition to considering the strength of the joint, whether the joint type requires penetration into the bamboo culm to secure it becomes vital for further connection design considerations.

CONCLUSIONS

1. The lateral partial compression test on bamboo culms determined that bamboo culms have four cracks upon breaking, and the presence of nodes can prevent a bamboo culm from cracking into four equal parts. Increasing the number of nodes and subsequently positioning them at the base of the bamboo culms can increase the ultimate load of the bamboo culm. There is no significant difference in ultimate load between mid-section and end- section specimen. According to the tensile test, all the three types of joint have elastic area in which they undergo loads and the tensile stiffness in the elastic region presents in following descending sequence: iron wire joint >lashing joint >steel bracket joint; the reverse is true for ultimate load.
2. The slip test indicates that the presence of bamboo node can effectively increase the slip stiffness and ultimate load of lashing and iron wire joints. Among the three joint types, the descending rank of slip stiffness shows the following sequence: steel bracket joint > lashing joint with node > steel bracket joint with node > lashing joint without node > iron wire joint without node. And the slipping ultimate load in descending order is: steel bracket joint > lashing joint with node > iron wire joint with node > lashing joint without node > iron wire joint without node.
3. Rotational stiffness of three joint types occurred in descending order as follows: steel bracket joint >lashing joint > iron wire joint. The resistance to rotation after deformation was highest in the steel bracket joint when compared to the other two types of joint.

ACKNOWLEDGEMENTS

This study was supported by a Grant (112-B03) from the Experimental Forest, College of Bioresource and Agriculture, National Taiwan University, Taiwan, ROC. The authors thank the Forestry Bureau for financial support.

Author Contributions

MJC and DYL designed the concept of the study. DYL performed the experiments and analyzed the data. MJC wrote the initial version of the paper, and CJL edited it through to the final version. Both CJL and MJT read and approved the final manuscript.

Competing Interests

The authors declare that they have no competing interests.

Availability of Data and Materials

The datasets used and/or analyzed during the current study are available from the corresponding author on reasonable request.

REFERENCES CITED

Ahmad, M., and Kamke, F. K. (2005). "Analysis of Calcutta bamboo for structural composite materials: Physical and mechanical properties," *Wood Science and Technology* 39, 449-459. DOI: 10.1007/s00226-005-0016-y

Amada, S., and Untao, S. (2001). "Fracture properties of bamboo," *Composites Part B: Engineering* 32(5), 451-459. DOI: 10.1016/S1359-8368(01)00022-1

Awaludin, A., and Andriani, V. (2014). "Bolted bamboo joints reinforced with fibers," *Procedia Engineering* 95, 15-21. DOI: 10.1016/j.proeng.2014.12.160

Chand, N., Shukla, M., and Sharma, M. K. (2008). "Analysis of mechanical behaviour of bamboo (*Dendrocalamus strictus*) by using FEM," *Journal of Natural Fibers* 5(2), 127-137. DOI: 10.1080/15440470801928970

Hong, C., Li, H., Xiong, Z., Lorenzo, R., Corbi, I., Corbi, O., Wei, D., Yuan, C., Yang, D., and Zhang, H. (2020). "Review of connections for engineered bamboo structures," *Journal of Building Engineering* 30, 101324-101337. DOI: 10.1016/j.jobe.2020.101324

Kobayashi, H., Daimaruya, M., and Oda, M. (1996). "Impact lateral compression test for circular ceramic tube; Ceramics enkan no shogeki yoko asshuku shiken," *Journal of the Society of Materials Science* 45(8), 901-906. ISSN 0514-5163

Lee, D.Y., Chung, M.J., and Tsai, M. J. (2020). "Exploring the mechanical behavior of cross-lap joint of *Phyllostachys makinoi* by rope lashing experiments," *Journal of the Experimental Forest of National Taiwan University* 34(1), 51-66. [in Chinese] DOI: 10.6542/EFNTU.202003_34(1).0005

Moran, R., Benitez, C., Sliva, H. F., and Garcia J. J. (2016). "Design of steel connectors for structural bamboo members," in: *International Conference on Advanced Mechatronics, Design, and Manufacturing Technology (AMDM)*, Cali, Colombia.

Obataya, E., Kitin, P., and Yamauchi, H. (2007). "Bending characteristics of bamboo (*Phyllostachys pubescens*) with respect to its fiber–foam composite structure," *Wood*

Science and Technology 41, 385-400. DOI: 10.1007/s00226-007-0127-8

Raj, A.D., and Agarwal, A.B. (2014). "Bamboo as a building material," *Journal of Civil Engineering and Environmental Technology* 1(3), 56-61. ISSN: 2349-879X

Vahanvati, M. (2015). "The challenge of connecting bamboo," in: *10th World Bamboo Congress*, Damyang, Korea.

Article submitted: February 28, 2024: Peer review completed: April 24, 2024; Revised version received: May 20, 2024; Accepted: August 15, 2024; Published: September 3, 2024.
DOI: 10.15376/biores.19.4.7911-7930